Nanopore-Based Conformational Analysis of a Viral RNA Drug Target

Carolyn Shasha,[§,†] Robert Y. Henley,[†,§] Daniel H. Stoloff,[†] Kevin D. Rynearson,[‡,⊥] Thomas Hermann,[‡] and Meni Wanunu[†,*]

[†]Departments of Physics and Chemistry/Chemical Biology, Northeastern University, Boston, Massachusetts 02115, United States, and [‡]Department of Chemistry and Biochemistry, University of California, San Diego, La Jolla, California 92093, United States. [§]These authors have contributed equally to this work. [⊥]Present address: Department of Neurosciences, UCSD.

ABSTRACT Nanopores are single-molecule sensors that show exceptional promise as a biomolecular analysis tool by enabling label-free detection of small amounts of sample. In this paper, we demonstrate that nanopores are capable of detecting the conformation of an antiviral RNA drug target. The hepatitis C virus uses an internal ribosome entry site (IRES) motif in order to initiate translation by docking to ribosomes in its host cell. The IRES is therefore a viable and important drug target. Drug-induced changes to the conformation of the HCV IRES motif, from a bent to a straight conformation, have been shown to inhibit HCV replication. However, there is presently no straightforward method to analyze the effect of candidate small-molecule drugs on the RNA conformation. In this paper, we show that RNA translocation dynamics through a 3 nm diameter nanopore is conformation-sensitive by demonstrating a difference in transport times between bent and straight conformations of a short viral RNA motif. Detection is possible because bent RNA is stalled in the 3 nm pore, resulting in longer molecular dwell times than straight RNA. Control experiments show that binding of a weaker drug does not produce a conformational change, as consistent with independent fluorescence measurements. Nanopore measurements of RNA conformation can thus be useful for probing the structure of various RNA motifs, as well as structural changes to the RNA upon small-molecule binding.

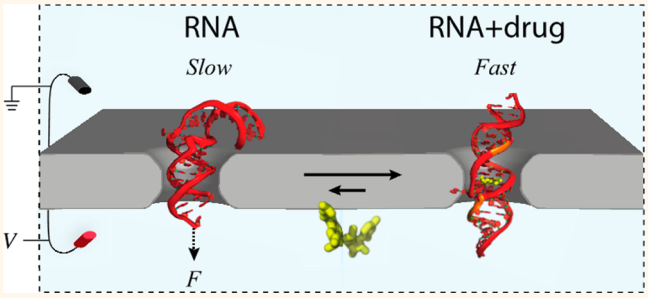

KEYWORDS: nanopores · RNA conformation · HCV · IRES · drug screening

Understanding the molecular basis of disease has enormously impacted health in our society by providing insightful paths to disease diagnosis and rational drug development. In recent years, isolation and interrogation of ribonucleic acid (RNA) molecules has revolutionized our view on biology. A prime example of this is that low abundance RNA molecules (*e.g.*, microRNA, long noncoding RNA) have been shown to exhibit diverse functional roles in cell maintenance. Similarly to proteins, RNA function is frequently connected to formation of an elaborate three-dimensional structure, and the ability to monitor conformation in RNA molecules has potential medicinal uses. For example, the hepatitis C virus (HCV) causes hepatitis C in humans, a life-threatening liver inflammation that occurs in roughly 80% of patients infected with HCV. There is currently no vaccine for HCV, and before the approval of direct antiviral drugs, leading treatments were only curative in 50% of patients.[1] HCV replicates by binding to host cell ribosomes using an internal ribosome entry site (IRES) RNA motif. The IRES domain is a highly conserved motif that allows efficient, cap-independent translation initiation at the ribosome by virtue of its elbow structure. The structures of subdomain IIa of the IRES element of HCV, as well as high and low affinity benzimidazole derivatives **1** and **2** that bind to it, are shown in Figure 1a. The L-shaped domain II of the HCV IRES is structurally similar to the 40S ribosomal subunit that it binds to,[2] and once deformed, the IRES is unable to attach to the host ribosome and replicate.

Many approaches for inhibiting IRES activity *in vivo* have been sought, including the use of anti-IRES aptamers[3] and small-molecule drugs. Recently, the Hermann group has shown that a benzimidazole derivative targets the IRES with micromolar affinity and by deforming its highly

* Address correspondence to wanunu@neu.edu.

Received for review April 8, 2014 and accepted May 26, 2014.

Published online May 26, 2014
10.1021/nn501969r

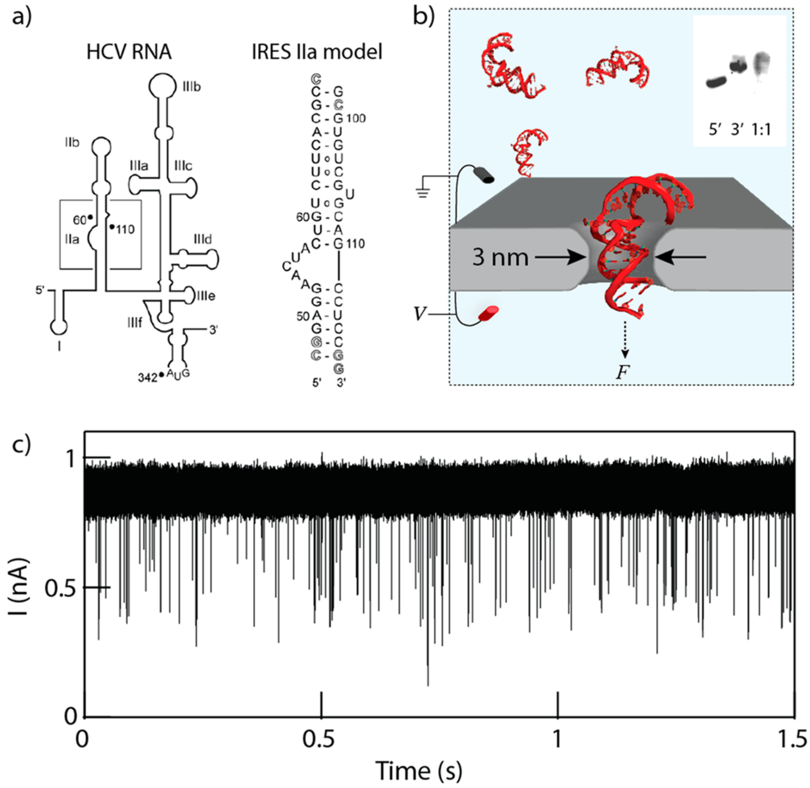

Figure 1. RNA conformational analysis using nanopores. (a) Cartoon map of the Hepatitis C (HCV) viral RNA. The box highlights the subdomain IIa, which adopts a bent fold within the internal ribosome entry site (IRES). A synthetic model of the IIa subdomain, consisting of two hybridized single-stranded RNAs. (b) Scheme of a 3 nm diameter pore in a 10 nm-thick silicon nitride (SiN_x) membrane, used to electrophoretically thread the RNA molecules. Inset shows PAGE gel image of the 5′ and 3′ RNA oligos and their 1:1 hybridized complex. (c) Continuous current *vs* time trace (top) of a 0.8 μM solution of the IRES IIa model in 0.3 M KCl, and a concatenated set of analyzed events from the same experiment (V = 200 mV, T = 25 °C, pH = 8.0, low-pass filter 200 kHz).

conserved structure, HCV RNA translation is efficiently inhibited.[4] This deformation has been verified by using nuclear magnetic resonance and Forster resonance energy transfer (FRET).[5] FRET is an effective tool for monitoring RNA conformations, as it reports on the distance between two fluorescent dyes conjugated at particular sites on the RNA molecule of interest. However, while FRET stands as a convenient method, the tedious need for chemical labeling of RNA makes RNA molecular preparation quite expensive. In addition, possible nucleic acid/dye interactions can impact the structure of the RNA of study, as well as interactions with the potential RNA binder. Therefore, a label-free method that can monitor changes in RNA conformation in real time without the need for chemical labels would aid in the search for various RNA targeting drugs.

In this paper, we show that nanopores can be used to detect the HCV IRES subdomain IIa conformational changes induced by benzimidazole derivatives. Nanopore sensing employs a voltage bias across the pore to electrophoretically drive individual macromolecules. The ion current produced by the voltage bias is used to measure biomolecular passage at high temporal resolution. Advantages of nanopores include label-free detection, single-molecule sensitivity, and the ability to detect biomolecules at attomole levels. These features make nanopores promising tools for screening drugs that induce conformational changes in viral RNA. Biological nanopores such as α-hemolysin have previously been utilized for studying nucleic acid conformations such as G-quadruplex structures,[6,7] aptamers to small molecules,[8,9] and DNA hairpins with chemical damage.[10,11] In addition, prior RNA detection works using nanopores include studies of the dynamics of single-stranded[12−15] and double-stranded[16] RNA translocations, microRNA and tRNA detection,[17] RNA/antibiotic interactions,[18] RNA/protein interactions,[19,20] RNA folding and secondary structures,[21] and have demonstrated nanopores sensitive enough to discriminate between different RNA homopolymers.[22] Solid-state nanopores, which offer the advantages of enabling a wider range of forces to be applied, a tunable pore geometry, and tunable pore surface chemistry have recently been used for studying the conformations of proteins.[23−25] However, to our knowledge, in this study we report the first use of synthetic pores for probing RNA conformational changes.

Our approach for detecting RNA conformational changes relies on solid-state nanopores of precise

geometry, which are used to discriminate bent from linear RNA conformations based on differences in translocation dynamics. Cartoon images of a 3 nm diameter nanopore and the HCV subdomain IIa RNA construct used in our experiments are shown in Figure 1b. Since RNA is negatively charged, applying a positive bias to the bottom chamber (*trans* chamber) provides an electrophoretic force (*F*) that pulls the RNA molecule through the pore. Transport of a bent molecule through the pore is hindered, while a linear conformation would translocate largely unhindered. In Figure 1c, a typical continuous current trace containing translocations of these RNA molecules is shown, along with several zoomed-in events expanded for visibility. A TEM image and current−voltage curve of a 3 nm diameter nanopore is shown in the Supporting Information (Figure S1).

The HCV IRES domain was reconstituted by heating a mixture of 400 μM 5′-CGG AGG AAC UAC UGU CUU CAC GCC and 5′-GCG UGU CGU GCA GCC UCC GG (Genscript, Piscataway, NJ) to 70 °C, followed by slow cooling to room temperature, as previously described.[5] Two drugs were used in this study, as shown in Figure 2a: positive control drug **1** has been shown using FRET to bind to the elbow region of the IRES domain with a dissociation constant of ~3 μM,[5] while negative control **2** is an analogue drug with a much weaker affinity of ~64 μM.[26] Therefore, in this study compound **1** serves as a positive control and compound **2** as a negative control. Binding and conformational change induced by compound **1** to the HCV RNA was confirmed by repeating the FRET assay performed by Parsons and co-workers (Figure 2b).[5] For this experiment, RNA oligos with identical sequences to those indicated above were used, with their 5′ ends labeled using Cy3 and Cy5. We performed the FRET assay with HCV in the presence of 300 mM KCl, an identical electrolyte as that used for the nanopore experiments. High K^+ concentrations are known to mimic divalent ion concentrations, and therefore no Mg^{2+} was required in our buffer. The decrease in FRET intensity with added drug confirms an increase in the interhelical angle of the RNA, which effectively changes its conformation from bent to straight.

Pores were assembled in a homemade PTFE cell using an elastomeric gasket to provide a good seal and reduce the device capacitance, which contributes to high-frequency noise.[27] A solution of 0.3 M KCl electrolyte tris-buffered to pH 8.0 was introduced to both sides of the chip such that the pore forms a solitary fluid channel between the two chambers. Before every experiment, the pore was checked for absence of "fake" pulses upon applying a voltage, which typically indicates pore contamination. Then, IRES RNA was added to a final concentration of 0.8 μM, and 30−60 s long continuous current traces were recorded at an applied voltage of 200 mV. For experiments with

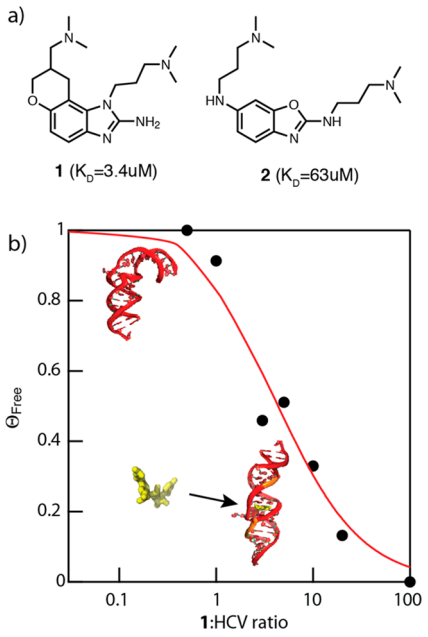

Figure 2. (a) Chemical structures of the high-affinity binder 1 (K_d = 3.4 μM) and negative control binder 2 (K_d = 64 μM). (b) FRET titration of 1 at 0.3 M KCl at different 1:HCV ratios, where the concentration of HCV RNA was 1.8 μM.

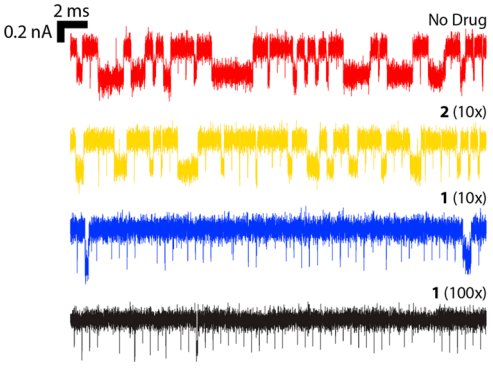

Figure 3. Concatenated traces that display 30−50 characteristic events for the different experiments. Each detected event is shown with 250 μs of data before and after the event.

RNA/drug mixtures, indicated numbers of molar equivalents were added to the RNA solution and mixtures were incubated for a minimum of 30 min prior to recording traces. Collected traces were then analyzed to extract transit dwell time t_d and mean current blockade amplitude ΔI for each pulse using the OpenNanopore program developed by the Radenovic group.[28]

RESULTS AND DISCUSSION

Nanopore experiments were performed on the complexes of RNA with compound **1** and compound **2** in order to demonstrate the sensitivity of nanopores to RNA conformation. Sample traces of concatenated events are shown in Figure 3, where the events are bunched after analysis with 250 μs shown before and

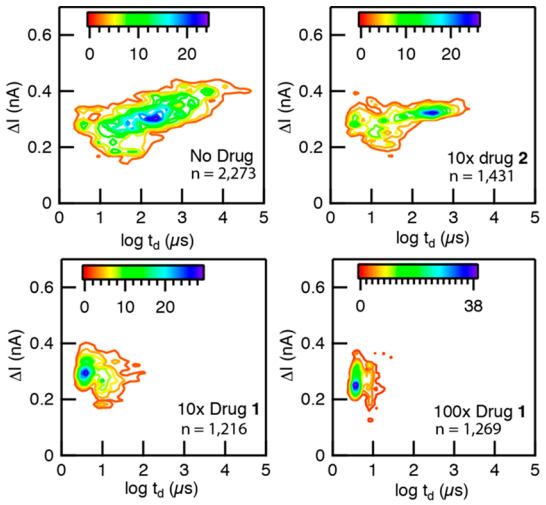

Figure 4. Contour plots of the log of the dwell time *vs* current blockage for various drug/HCV ratios, where IRES HCV RNA concentration was maintained at 0.8 μM in all experiments (3 nm diameter pore, V = 200 mV). Number of events (n) indicated in each contour plot.

after every detected event. As seen in the traces, in the absence of drug, pulses with a broad range of durations are observed, up to the millisecond regime. Similarly, for 10× control drug **2**, we observe a wide range of events. However, upon the addition of 10× and 100× drug **1**, long events are virtually absent, and we notice an exclusive set of short pulses with average translocation times below 10 μs.

The collective behavior of >1000 events in each experiment is represented by the contour plots of current blockade amplitudes ΔI *vs* dwell times t_d for the different experiments is shown in Figure 4. Pulse durations are shown in log scale in order to capture the breadth of dwell times for the free RNA molecule. This breadth is due to the fact that the molecule has to deform in order to "squeeze" through the 3 nm pore constriction, an activated process that generally has a broad distribution of times for weak applied forces (see voltage study in the Supporting Information, Figure S2). The most abundant region of the distribution of events clearly shifts from $\sim 10^{2.5}$ μs in the absence of drug to $\sim 10^{1}$ μs when **1** is present, reflecting a significant overall reduction in the dwell time of events in the presence of **1**. These short events upon drug binding and RNA conformational change would be difficult to detect without the Chimera high-bandwidth amplifier (see data reproduction using two other pores using an Axopatch amplifier in Supporting Information, Figure S3).

From the contour plots in Figure 4, we also clearly see a correlation between the magnitude of current blocked and the RNA conformation: events longer than 100 μs for the free RNA tend to block a larger magnitude of current. As drug is added, the average current blockage decreases as the rate of long events drops. This is consistent with our expectation, as a bent RNA

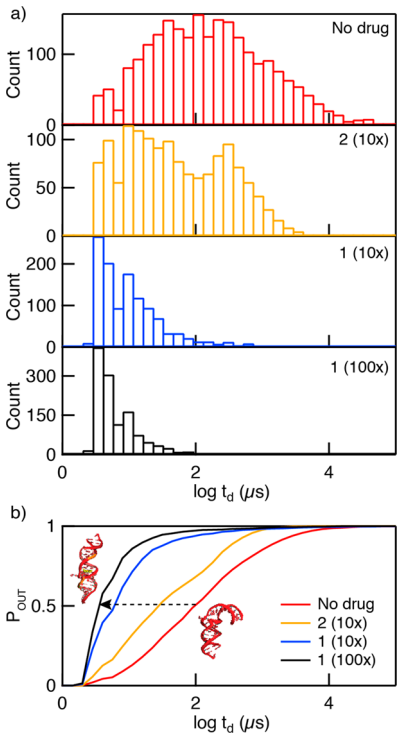

Figure 5. (a) Log dwell-time (t_d) histograms for the various experiments shown in Figure 3. (b) Integrated normalized dwell-time distributions, which highlight the shorter lifetime of the straight RNA conformation that results from drug binding to HCV RNA.

molecule trapped in the pore should block a larger fraction of ions than a straight molecule.

Dwell-time distributions are shown in Figure 5a (see analysis of dwell time distributions in Supporting Information, Figure S4). While characteristic dwell times for free RNA lie in a broad range of 0.1−10 ms, binding to **1** results in a pronounced decrease in dwell times to <0.1 ms, which agrees with the independent FRET results that confirm an RNA conformational change upon drug binding. In contrast to the results obtained for drug **1**, the experiment with 10x compound **2** on the same pore did not produce a noticeable change, and the population of longer translocations is still visible (similar to free HCV RNA).

Finally, Figure 5b shows integrated (and normalized) dwell-time distributions for the experiments shown in Figure 3. The curves display the probability of RNA translocation with time. Since our nanopore has a diameter of 3 nm, which just accommodates an RNA duplex, the probability of transporting a bent RNA conformation rises moderately with time, as indicated by the red curve which shows a small slope in the P_{out} *vs* dwell time. In contrast, the conformational change induced by compound **1** binding sharply increases the translocation probability at early times, which indicates that the molecule experiences no hindrance upon translocation through the pore.

CONCLUSION

We have shown that a ~3 nm diameter nanopore is a viable label-free detector of RNA conformational

change. HCV IRES subdomain IIa is a viable RNA drug target because it is required for HCV virus replication. Binding of the IRES motif to benzimidazole derivative **1** results in a sharp conformational change.[5] This change was readily detected by measuring RNA translocation times. Despite the small size of the HCV IRES domain IIa, which is approximately equivalent to a ~25 base pair fragment in length,[29] 3 nm diameter nanopores easily distinguish straight from bent RNA conformations. Experiments using larger pores and/or using higher applied voltage (not shown) lead to fast pulses for the IRES domain IIa that are indistinguishable from its complex with **1**. This ability of nanopores to probe conformational changes in unlabeled RNA points toward the possibility of using nanopores to screen for drugs that induce conformational changes to RNA targets, particularly for ones in which chemical labeling is not a viable approach, or when only small amounts of material are available.

MATERIALS AND METHODS

Nanopores were fabricated on ~20 nm thick silicon nitride freestanding membranes supported by a Si chip using a JEOL 2010FEG transmission electron microscope, as previously described.[30] Fabricated nanopores were cleaned using hot piranha solution and following a copious rinse with deionized water, they were assembled in a custom PTFE cell equipped with homemade Ag/AgCl electrodes.

The domain IIa model was reconstituted using supplied oligos according to the Hermann group.[5] To perform fluorescence imaging, we used supplies oligos to which fluorophores were attached on either end. We made titrations of HCV and the drug benzimidazole in TEX buffer in both water and 0.3 M KCl. FRET was performed in a real-time PCR instrument (Bio-Rad CFX96) by preparing solutions of 1.8 μM HCV and varying the HCV:drug ratio up to 1:100, in accordance with Hermann's group.

For nanopore experiments, we reconstituted the domain IIa by 1:1 hybridization of unlabeled RNA oligos using an identical melting-annealing step as with labeled oligos (gel image that confirms hybridization is shown the inset to Figure 1b). Nanopore experiments were performed by titrating drug sample into 0.8 μM RNA in 0.3 M KCl electrolyte buffered to pH 8.0 using Tris. All nanopore experiments were performed at room temperature. A 200 mV voltage was applied to the collection (*trans*) chamber of the nanopore using a pair of Ag/AgCl electrodes. Data was acquired at 4.19 MHz using a Chimera Instruments VC100 and prior to analysis it was low-pass filtered at 200 kHz to provide a suitable signal-to-noise ratio. Analysis of the traces was performed using a modified version of the open-source OpenNanopore MATLAB program developed by Raillon,[28] which utilizes a cumulative sums algorithm for pulse detection.

Conflict of Interest: The authors declare no competing financial interest.

Supporting Information Available: Details on pore characteristics; dwell time distributions for HCV RNA; and HCV RNA voltage dependence study. This material is available free of charge *via* the Internet at http://pubs.acs.org.

Acknowledgment. Spencer Carson is gratefully acknowledged for nanopore fabrication and for valuable comments on the manuscript.

REFERENCES AND NOTES

1. Torresi, J.; Johnson, D.; Wedemeyer, H. Progress in the Development of Preventive and Therapeutic Vaccines for Hepatitis C Virus. *J.Hepatol.* **2011**, *54*, 1273–1285.
2. Spahn, C. M.; Kieft, J. S.; Grassuci, R.; Penczek, P.; Zhou, K.; *et al.* Hepatitis C Virus Ires RNA-Induced Changes in the Conformation of the 405 Ribosomal Subunit. *Science* **2001**, *291*, 1959–1962.
3. Kikuchi, K.; Umehara, T.; Fukuda, K.; Kuno, A.; Hasegawa, T.; *et al.* A Hepatitis C Virus (HCV) Internal Ribosome Entry Site (Ires) Domain III–IV-Targeted Aptamer Inhibits Translation by Binding to an Apical Loop of Domain IIId. *Nucleic Acids Res.* **2005**, *33*, 683–692.
4. Zhou, S.; Rynearson, K. D.; Ding, K.; Brunn, N. D.; Hermann, T. Screening for Inhibitors of the Hepatitis C Virus Internal Ribosome Entry Site RNA. *Bioorg. Med. Chem.* **2013**, *21*, 6139–6144.
5. Parsons, J.; Castaldi, M. P.; Dutta, S.; Dibrov, S. M.; Wyles, D. L.; *et al.* Conformational Inhibition of the Hepatitis C Virus Internal Ribosome Entry Site RNA. *Nat. Chem. Biol.* **2009**, *5*, 823–825.
6. Shim, J. W.; Gu, L.-Q. Encapsulating a Single G-Quadruplex Aptamer in a Protein Nanocavity. *J. Phys. Chem. B* **2008**, *112*, 8354–8360.
7. Shim, J.; Gu, L. Q. Single-Molecule Investigation of G-Quadruplex Using a Nanopore Sensor. *Methods* **2012**, *57*, 40–46.
8. Ying, Y.-L.; Wang, H.-Y.; Sutherland, T. C.; Long, Y.-T. Monitoring of an ATP-Binding Aptamer and Its Conformational Changes Using an α-Hemolysin Nanopore. *Small* **2011**, *7*, 87–94.
9. Arnaut, V.; Langecker, M.; Simmel, F. C. Nanopore Force Spectroscopy of Aptamer-Ligand Complexes. *Biophys. J.* **2013**, *105*, 1199–1207.
10. Jin, Q.; Fleming, A. M.; Burrows, C. J.; White, H. S. Unzipping Kinetics of Duplex DNA Containing Oxidized Lesions in an A-Hemolysin Nanopore. *J. Am. Chem. Soc.* **2012**, *134*, 11006–11011.
11. An, N.; Fleming, A. M.; White, H. S.; Burrows, C. J. Crown Ether-Electrolyte Interactions Permit Nanopore Detection of Individual DNA Abasic Sites in Single Molecules. *Proc. Natl. Acad. Sci. U.S.A.* **2012**, *109*, 11504–11509.
12. Kasianowicz, J.; Brandin, E.; Branton, D.; Deamer, D. Characterization of Individual Polynucleotide Molecules Using a Membrane Channel. *Proc. Natl. Acad. Sci. U.S.A.* **1996**, *93*, 13770–13773.
13. Butler, T. Z.; Gundlach, J. H.; Troll, M. A. Determination of RNA Orientation during Translocation through a Biological Nanopore. *Biophys. J.* **2006**, *90*, 190–199.
14. van den Hout, M.; Skinner, G. M.; Klijnhout, S.; Krudde, V.; Dekker, N. H. The Passage of Homopolymeric Rna through Small Solid-State Nanopores. *Small* **2011**, *7*, 2217–2224.
15. Cracknell, J. A.; Japrung, D.; Bayley, H. Translocating Kilobase Rna through the Staphylococcal Alpha-Hemolysin Nanopore. *Nano Lett.* **2013**, *13*, 2500–2505.
16. van den Hout, M.; Vilfan, I. D.; Hage, S.; Dekker, N. H. Direct Force Measurements on Double-Stranded RNA in Solid-State Nanopores. *Nano Lett.* **2010**, *10*, 701–707.
17. Wanunu, M.; Dadosh, T.; Ray, V.; Jin, J.; McReynolds, L.; *et al.* Rapid Electronic Detection of Probe-Specific Micrornas Using Thin Nanopore Sensors. *Nat. Nano* **2010**, *5*, 807–814.
18. Wanunu, M.; Bhattacharya, S.; Xie, Y.; Tor, Y.; Aksimentiev, A.; *et al.* Nanopore Analysis of Individual RNA/Antibiotic Complexes. *ACS Nano* **2011**, *5*, 9345–9353.
19. Lin, J.; Fabian, M.; Sonenberg, N.; Meller, A. Nanopore Detachment Kinetics of Poly(a) Binding Proteins from Rna Molecules Reveals the Critical Role of C-Terminus Interactions. *Biophys. J.* **2012**, *102*, 1427–1434.
20. Niedzwiecki, D. J.; Iyer, R.; Borer, P. N.; Movileanu, L. Sampling a Biomarker of the Human Immunodeficiency Virus across a Synthetic Nanopore. *ACS Nano* **2013**, *7*, 3341–3350.
21. Bundschuh, R.; Gerland, U. Coupled Dynamics of RNA Folding and Nanopore Translocation. *Phys Rev. Lett.* **2005**, *95*, No. 208104.

22. Akeson, M.; Branton, D.; Kasianowicz, J. J.; Brandin, E.; Deamer, D. W. Microsecond Time-Scale Discrimination among Polycytidylic Acid, Polyadenylic Acid, and Polyuridylic Acid as Homopolymers or as Segments within Single Rna Molecules. *Biophys. J.* **1999**, *77*, 3227–3233.
23. Talaga, D. S.; Li, J. L. Single-Molecule Protein Unfolding in Solid State Nanopores. *J. Am. Chem. Soc.* **2009**, *131*, 9287–9297.
24. Tavassoly, O.; Lee, J. S. Methamphetamine Binds to Alpha-Synuclein and Causes a Conformational Change Which Can Be Detected by Nanopore Analysis. *FEBS Lett.* **2012**, *586*, 3222–3228.
25. Freedman, K. J.; Haq, S. R.; Edel, J. B.; Jemth, P.; Kim, M. J. Single Molecule Unfolding and Stretching of Protein Domains inside a Solid-State Nanopore by Electric Field. *Sci. Rep.* **2013**, *3*, 1638.
26. Rynerason, K. D.; Charrette, B.; Gabriel, C.; Moreno, J.; Boerneke, M. A.; Dibrov, S. M; Hermann, T. 2-Aminobenzoxazole ligands of the hepatitis C virus internal ribosome entry site. *Bioorg. Med. Chem. Lett.* **2014**, DOI: 10.1016/j.bmcl.2014.05.088.
27. Tabard-Cossa, V.; Trivedi, D.; Wiggin, M.; Jetha, N. N.; Marziali, A. Noise Analysis and Reduction in Solid-State Nanopores. *Nanotechnology* **2007**, *18*, 305505.
28. Raillon, C.; Granjon, P.; Graf, M.; Steinbock, L. J.; Radenovic, A. Fast and Automatic Processing of Multi-Level Events in Nanopore Translocation Experiments. *Nanoscale* **2012**, *4*, 4916–4924.
29. Lukavsky, P. J.; Otto, G. A.; Lancaster, A. M.; Sarnow, P.; Puglisi, J. D. Structures of Two RNA Domains Essential for Hepatitis C Virus Internal Ribosome Entry Site Function. *Nat. Struct. Biol.* **2000**, *7*, 1105–1110.
30. Kim, M. J.; Wanunu, M.; Bell, D. C.; Meller, A. Rapid Fabrication of Uniformly Sized Nanopores and Nanopore Arrays for Parallel DNA Analysis. *Adv. Mater.* **2006**, *18*, 3149–3155.